arXiv:1210.2365v1 [astro-ph.CO] 8 Oct 2012

Determination of the abundance of cosmic matter via the cell count moments of the galaxy distribution

J. Bel[1] and C. Marinoni[1,2]
[1]Centre de Physique Théorique, Aix-Marseille Univ., UMR 7332, F-13288 Marseille, France
[2]Institut Universitaire de France, 103, bd. Saint-Michel, F-75005 Paris, France

(Dated: October 9, 2012)

We demonstrate that accurate and precise cosmological information can be extracted from the cell count analysis of the 3D spatial clustering of galaxies once the second-order ratio between one- and two-point moments of the smoothed galaxy density distribution is analyzed. This probe does not require the calibration of any standard rod, the knowledge of the galaxy bias nor the modeling of galaxy redshift distortions. Using the spectroscopic Sloan Digital Sky Survey (SDSS) data release 7 (DR7) galaxy sample, no cosmic microwave background (CMB) information, weak (flat) priors on the value of the curvature of the universe (Ω_k) and the constant value of the dark energy equation of state (w), we estimate the abundance of matter (Ω_m) with a relative error of 11% (at 68% c.l.). The method may be instrumental in searching for evidences of new physics beyond the standard model of cosmology and in planning future missions such as BigBOSS or EUCLID.

PACS numbers:

Determining the value of the constitutive parameters of the Friedman equations is a problem of great observational and interpretative difficulty, but owing to its bearing on fundamental physics, is one of great theoretical significance. This challenge can be addressed through the development of performant cosmic probes, sophisticated error analysis schemes, and formidable observational programs from both ground and space [1]. The Wilkinson microwave anisotropy probe (WMAP), for example, fix with impressive accuracy the parameters of a 'power-law ΛCDM' model [2]. This is a cosmological model characterized by a flat geometry, a positive dark energy (DE) component Ω_X with $w = -1$, and by primordial perturbations that are scalar, Gaussian and adiabatic [3]. Notwithstanding, other astrophysical probes are needed if we are to constrain deviations from this minimal model [4]. Different approaches, being sensitive to different sets of nuisance parameters and to different subsets of the full cosmological parameter set, provides consistency checks, lift parameter degeneracies, enable stronger constraints and, in the end, a safer theoretical interpretation.

We characterize the inhomogeneous distribution of galaxies in terms of the local dimensionless density contrast $\delta_g(\mathbf{x}) \equiv \rho_g(\mathbf{x})/\langle\rho_g(\mathbf{x})\rangle - 1$, where $\rho_g(\mathbf{x})$ is the comoving density of galaxies in configuration space, and where $\langle\rho_g(\mathbf{x})\rangle$ denotes the selection function, the expected mean number of galaxies at position $\mathbf{x}$ given the selection criteria of the survey. Since the galaxy distribution is a stochastic point process, a spherical top-hat filter W of radius R is applied to generate a continuous, coarse-grained observable $\delta_{g,R}(\mathbf{x}) = \int \delta(\mathbf{y})W(|\mathbf{x}-\mathbf{y}|/R)d\mathbf{y}$. The 1-point $\kappa_{20,g,R} = \langle\delta^2_{g,R}(\mathbf{x})\rangle_c$ and the 2-point $\kappa_{11,g,R}(\mathbf{r}) = \langle\delta_{g,R}(\mathbf{x})\delta_{g,R}(\mathbf{x}+\mathbf{r})\rangle_c$ cumulant moments are the lowest-order non-zero connected moments of the probability distribution functional (PDF) of the field $\delta_{g,R}(\mathbf{x})$ [5–7]. If the PDF is stationary and isotropic, the quantity $\kappa_{11,g,R}(\mathbf{r})/\kappa_{20,g,R}$ reduces to the ratio between the correlation function and the variance of the filtered field

$$\eta_{g,R}(r,\mathbf{p}) = \frac{\xi_{g,R}(r,\mathbf{p})}{\sigma^2_{g,R}(\mathbf{p})}, \tag{1}$$

where we have explicitly emphasized the dependence of the observable on the set $(\mathbf{p})$ of cosmological parameters. This comes trough because the LHS term of eq. (1) can be estimated from data only once a comoving distance-redshift conversion model is supplied.

It is straightforward to predict the value of the second-order galaxy clustering ratio $\eta_{g,R}$. On sufficiently large cosmic scales R, matter fluctuations are small and described by the linear power spectrum $\Delta^2_L(k,\mathbf{p}) = 4\pi A k^{n_s+3}T^2(k,\mathbf{p})$, where A is a normalization factor, n_s is the primordial spectral index, and T^2 is the transfer function [8]. Accordingly, the amplitudes of the second-order statistics for mass evolve as a function of redshift (z) and scale as $\sigma^2_R(z,\mathbf{p}) = \sigma^2_8(z=0)D^2(z)\mathcal{F}_R(\mathbf{p})$, and $\xi_R(r,z,\mathbf{p}) = \sigma_8(z=0)^2D^2(z)\mathcal{G}_R(r,\mathbf{p})$. Both these equations are normalized at the scale $r_8 = 8h^{-1}$Mpc, $D(t)$ represents the linear growing mode [3], while the effects of filtering are incorporated in the functions

$$\mathcal{F}_R(\mathbf{p}) = \frac{\int_0^{+\infty}\Delta^2_L(k,\mathbf{p})\hat{W}^2(kR)d\ln k}{\int_0^{+\infty}\Delta^2_L(k,\mathbf{p})\hat{W}^2(kr_8)d\ln k} \tag{2}$$

$$\mathcal{G}_R(r,\mathbf{p}) = \frac{\int_0^{+\infty}\Delta^2_L(k,\mathbf{p})\hat{W}^2(kR)\frac{\sin(kr)}{kr}d\ln k}{\int_0^{+\infty}\Delta^2_L(k,\mathbf{p})\hat{W}^2(kr_8)d\ln k} \tag{3}$$

where $\hat{W}$ is the Fourier transform of the window function.

By analogy, we define the mass clustering ratio which is explicitly given by

$$\eta_R(r,\mathbf{p}) = \frac{\mathcal{G}_R(r,\mathbf{p})}{\mathcal{F}_R(\mathbf{p})}. \tag{4}$$

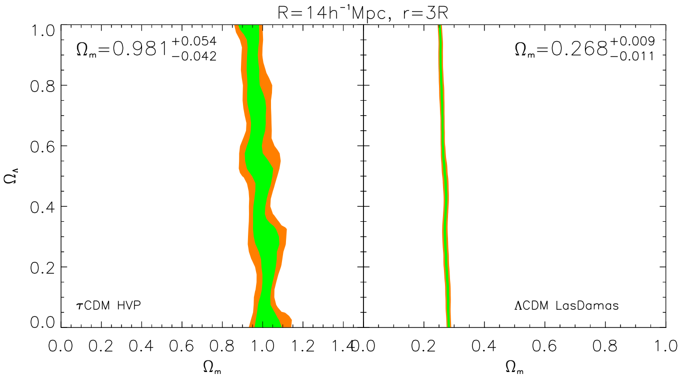

FIG. 1: *Left panel:* two-dimensional confidence limits on Ω_m and Ω_Λ from a 'blind' analysis of the τCDM HVP simulation [11]. This synthetic catalog of clusters of galaxies covers one octant of sky, extends over the redshift interval $0.1 < z < 0.43$, is comprised of $\sim 10^6$ massive halos with an average space density of $6 \times 10^{-4} h^3 \mathrm{M}pc^{-3}$ and it was simulated using $\mathbf{p}^i = (1,\ 0,\ -1,\ 21,\ 0,\ 1)$. Contours are plotted for $\mathcal{L}/\mathcal{L}_{min} < 2.3, 6.17$ corresponding to 68 and 95 per cent *c.l.* for a multivariate Gaussian distribution with 2 degrees of freedom. The relevant one-dimensional marginalized constraint is shown in the inset. The clustering ratio $\eta_{g,R}(r, \mathbf{p})$ is estimated using $R = 14h^{-1}\mathrm{M}pc$ and $r = 3R$. For the best fitting cosmology we measure $\eta_{g,R}(r, \mathbf{p}^f) = 0.0294 \pm 0.0017$ where the error is evaluated via 30 jackknife resampling of the data, excluding each time a sky area of 36×19.5 deg^2. Dirac delta priors are taken of $\Omega_b h^2$, H_0 and n_s, that are centered on the simulated values. *Right panel:* same as before, but now contours represent the joint likelihood analysis of 40 independent ΛCDM mock catalogs simulating the SDSS LRG sample. Each of these simulations covers 120×45 deg^2, extends over the redshift interval $0.16 < z < 0.43$, is comprised of ~ 60000 galaxies with an average space density of $\sim 8.9 \times 10^{-5} h^3 \mathrm{M}pc^{-3}$ and the input cosmological parameters are $\mathbf{p}^i = (0.25,\ 0.75,\ -1,\ 70,\ 0.0196,\ 1)$. For the best fitting cosmology we find $\eta_{g,R}(r, \mathbf{p}^f) = 0.0573 \pm 0.0010$, where the error, computed as the *s.d.* of the mean of 40 measurements, includes the contribution from cosmic variance.

As long as a linear matter power spectrum is assumed, η_R is stable across cosmic time, *i.e.* it does not evolve as a function of redshift. Moreover, it is independent from the amplitude of the matter power spectrum normalization parameter A and it is also insensitive to the shape of the sample selection function, if the density gradient is nearly constant on scales $\sim 2R$.

Interestingly, eq. (4) is also unaffected by redshift distortions, and, therefore, independent of their specific modeling, that is the ratio $\eta_R(r, \mathbf{p})$ between second-order statistics has identical amplitude in both configuration- and real-space. If the only net effect of peculiar velocity is the enhancement of the amplitudes of the density ripples in Fourier space, without any change in their phases or frequencies, then redshift distortions equally contributes to the numerator and denominator of eq. (4). For any given R and r, hence, the ratio $\eta_R(r, \mathbf{p})$ behaves as a cosmic 'standard of clustering'.

The relationship between the mass and galaxy clustering ratios in configuration space follows immediately once we specify how well the overall matter distribution is traced by its luminous subcomponent on a given scale R. By adopting an arbitrary local non-linear biasing scheme, namely $\delta_{g,R}(\mathbf{x}) = \sum_{i=0}^{N} (b_i/i!)\delta_R^i(\mathbf{x})$, and in the limit $\sigma_{g,R}^2 << 1$, we obtain [7]

$$\eta_{g,R}(r, \mathbf{p}) = \eta_R(r, \mathbf{p}), \tag{5}$$

an identity that is independent of the specific value of the bias amplitudes b_i. On scales $R > 10h^{-1}\mathrm{Mpc}$ and $r = 3R$, the approximation (5) is good to better than 0.5%, and to better than 0.1% on scales larger than $15h^{-1}\mathrm{Mpc}$ (for the same correlation length $r = 3R$).

As for a classical Alcock and Paczynski test [9], the equivalence expressed by eq. (5) holds true if and only if the LHS and RHS are both estimated in the correct cosmology. This is the principle that we exploit to constrain the value of key cosmological parameters. In this respect, we note that the RHS of eq. (5) is directly sensitive to the shape (n_s) of the primordial power spectrum of density fluctuations, as well as to the parameters determining the size of the horizon scale at matter-radiation equality (the present-day extrapolated value of the matter ($\Omega_m h^2$) and baryon ($\Omega_b h^2$) density parameters. The possible contribution of massive neutrinos is neglected in this analysis.) By contrast, the LHS term of eq. (5) probes the structure of the comoving distance-redshift relation, and, on top of Ω_m, it is also sensitive to Ω_X and w, *i.e.* to a wide range of DE models. Note that if distances are expressed in units of $h = H_0/100$, the LHS is effectively independent from the value of the Hubble constant H_0.

An additional merit of eq. (5) is the neat distinction in the physics that is brought about by its two terms. The LHS is a geometric probe since it is fully specified once the homogeneous expansion rate history of the universe is known. The nature of the RHS, instead, is fundamentally dynamical and it can be computed only when a specific gravitational theory is provided. If the expansion rate of the universe is independently known, one can therefore test whether general relativity correctly describes the formation of correlated structures in the universe. Such a strategy complements other approaches exploiting redshift distortion effects (*e.g.* [10]).

We estimate $\sigma_{g,R}^2$ and $\xi_{g,R}$ and correct measurements for shot noise effects according to the method detailed in [7]. Here, we describe how we evaluate $P(\mathbf{p}|\eta_{g,R})$, the likelihood of the unknown set of parameters $\mathbf{p} = (\Omega_m, \Omega_X, w, H_0, \Omega_b h^2, n_s)$ given the actual value of the observable $\eta_{g,R}$. Note that the analysis does not require the specification of further model parameters other than those quoted above. Since $\eta_{g,R}$ is approximately Gaussian, the most likely set ($\mathbf{p}^f$) is the one that minimizes the logarithmic posterior $\mathcal{L} = -\log P$

$$\mathcal{L} = \sum^{N} \log \sigma_{\eta,i} + \frac{\chi^2}{2} - \log \pi + B, \tag{6}$$

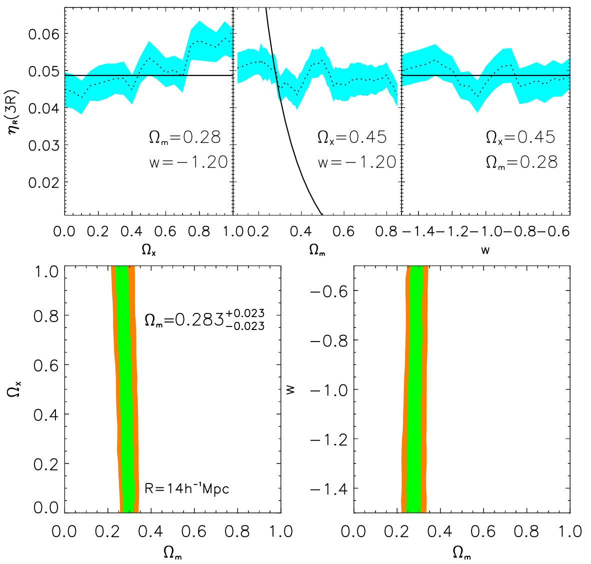

FIG. 2: *Upper panels:* The galaxy clustering ratio $\eta_{g,R}(r, \Omega_m, \Omega_X, w)$ (dotted line) reconstructed from SDSS DR7 data assuming $R = 14h^{-1}$Mpc and $r = 3R$ is plotted as a function of Ω_Λ (left), Ω_m (center) and w (right), after fixing the remaining cosmological parameters, shown in the inset, to the values that minimize the logarithmic posterior (6). Grey shading is the 1-sigma deviation around the mean and it is computed from 30 jackknife resampling of the data, excluding, each time, a sky area of 12×14 deg^2. This uncertainty is in good agreement ($< 10\%$ difference) with the standard deviation displayed by the 40 SDSS-like simulations LasDamas. We also show the predicted scaling of the mass clustering ratio (solid line) in the corresponding cosmology. The correct set of cosmological parameters is the very one that makes the two curves converge to the same numerical value. For these data we find $\eta_{g,R}(r, \mathbf{p}^f) = 0.0502 \pm 0.0036$. *Lower panels:* two-dimensional marginalized constraints on a curved XCDM model in which both Ω_X and w are allowed to vary. Gaussian priors are taken of $\Omega_b h^2 = 0.0213 \pm 0.0010$, of $H_0 = 73.8 \pm 2.4$ and of $n_s = 0.96 \pm 0.014$ from BBN [18], HST [19] and WMAP7 [2] determinations respectively. Contours are plotted for $\mathcal{L}/\mathcal{L}_{min} < 2.3, 6.17$.

where $\chi^2 = \sum^N \sigma_{\eta,i}^{-2}(\eta_{g,R} - \eta_R)^2$, where N is the number of estimates of $\eta_{g,R}$, $\sigma_{\eta,i}$ is the error on the observable, π describes any a-priori information about the PDF of $\mathbf{p}$, and where B is a normalization constant that can be fixed by requiring $\int P d\mathbf{p} = 1$. Since eq. (5) is free from look-back time effects, the analysis does not require slicing the sample in arbitrary redshift bins; only one estimation ($N = 1$) of eq. (1) is needed across the whole sample volume. We have recalculated the observable $\eta_{g,R}(r, \mathbf{p})$ for each comoving distance-redshift model, *i.e.* on a grid (Ω_m, Ω_X, w) of spacing $[10^{-2}, 5\cdot10^{-2}, 5\cdot10^{-2}]$. As a consequence, the posterior $\mathcal{L}$ does not vary smoothly between different models because the number of galaxies counted in any given cell varies from model to model. However, since the computation of the observable $\eta_{g,R}(3R, \mathbf{p})$ takes a limited amount of time, shot-noise is the price we have decided to pay in order to obtain an unbiased likelihood hyper-surface.

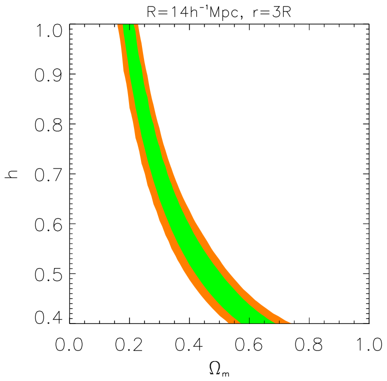

FIG. 3: Two-dimensional marginalized constraints on Ω_m and H_0 obtained by fitting data with a curved XCDM model. Contours are plotted for $\mathcal{L}/\mathcal{L}_{min} < 2.3, 6.17$ Gaussian priors are taken of $\Omega_b h^2 = 0.0213 \pm 0.0010$ and $n_s = 0.96 \pm 0.014$ from BBN [18] and WMAP7 [2] determinations respectively.

We test the performances of our method under realistic operating conditions via a 'blind' analysis of mock catalogs that are characterized by widely different sets of expansion rate and power spectrum parameters, mass tracers and radial selection functions. These are the τCDM Hubble Volume Project (HVP) simulation [11] and the LasDamas simulation [12]. An end-to-end analysis of clusters mock data (HVP) allows us to check for the presence of insidious algorithmic biases that could arise when training a method to 'recognize' only a fiducial ΛCDM cosmology via a single class of biased tracer of the matter clustering pattern, namely galaxies. The left panel of FIG. 1 shows that the input value $\Omega_M = 1$ is statistically retrieved. By a joint analysis of 40 ΛCDM mock catalogs that incorporate all the observing selections of the SDSS luminous red galaxies (LRG) survey, *i.e.* the Oriana output of the LasDamas simulations, we have verified that the specific SDSS observing biases do not spoil our cosmological inferences. The encouraging outcome of this analysis is presented in FIG. 1, and shows that redshift data in a volume 40 times larger than that probed by the SDSS DR7 LRG sample (still $\sim 10\%$ of those that will be measured by surveys such as EUCLID [15] or BigBOSS [16]) can constrain Ω_m precisely ($\sim 3.7\%$) and accurately (the input value is recovered). The strong sensitivity to the abundance of matter essentially arises because the zero order spherical Bessel function in eq. (3) filters in different portions of Δ_L^2 when Ω_m is changed. If we bias high Ω_m, the suppression of power in $\xi_R(r, \mathbf{p})$ on a scale r is larger than that observed when estimating $\xi_{g,R}(r, \mathbf{p})$ using the corresponding wrong distance-redshift relation (see FIG. 2). Concerning DE parameters, and as for other clustering probes (e.g. [13, 14]), constraints are not yet tight enough to yield a sensible measurement.

Turning to real data, the geometry of the SDSS DR7 subsample [17] is dictated by the need of sampling the galaxy distribution with cells of radius R as well as of correlating cell counts on scales r. The inferior limit on R is set by a theoretical constraint. Although not mandatory, the analysis is performed in the linear domain, so as to avoid any phenomenological description of the matter power spectrum. The choice of R, is additionally conditioned by the practical requirement of minimizing the shot noise contribution in each cell, *i.e.* $R > (4\pi\rho/3)^{-1/3}$. In this work we adopt the scale $R = 14h^{-1}$Mpc. The inferior limit $r = 3R$ in the correlation scale, instead, is set to guarantee optimal accuracy in the approximation (5). At the opposite end, the larger the values of R and r, and the less informative are the inferred cosmological predictions. The sample that complies with these constraints covers the redshift interval $0.15 < z < 0.43$, a contiguous sky area of 120×45 deg^2, is comprised of 62,652 LRG, and has a mean density of $9.2 \times 10^{-5} h^3 \mathrm{M}pc^{-3}$.

Without fixing neither the curvature of the universe (flat prior $0 < |\Omega_k| < 1$) nor the quality of the DE component (flat prior $-1/2 < w < -3/2$), but taking (strong) Gaussian priors of $\Omega_b h^2$, H_0 and n_s from big bang nucleosynthesis (BBN)[18], Hubble Space Telescope (HST)[19], and WMAP [2] respectively, data constrain the overall matter abundance with a precision of 8% (see FIG. 2, for the sake of completeness, by choosing a smoothing scale of $18/22h^{-1}$Mpc we obtain $0.270^{+0.037}_{-0.027}/0.255 \pm 0.038$.) This figure improves by a factor of two the estimate ($\Omega_m = 0.259 \pm 0.039$) obtained by analyzing, with the same priors, the large scale clustering (LSC) of the SDSS DR5 sample (which contains 25% less galaxies than DR7)[20]. It also improves by $\sim 20\%$ the constraint ($\Omega_m = 0.24^{+0.025}_{-0.024}$) of [13] obtained by combining LSC results from the DR7 sample with the full likelihood of the WMAP5 data [21] and a strong HST prior [22]. The relative precision achieved with our method compares with that ($\Omega_M = 0.294 \pm 0.023$) obtained by [23] by combining the LSC likelihood from the DR9 sample (containing 5 times more LRGs than the DR7 catalog) with the full likelihood of CMB data (WMAP7 [2]).

Interestingly, the best fitting value of Ω_m still remains within the quoted 68% c.l. even when we relax some of the strong priors. With a (weak) flat prior on n_s (in the interval $[0.9, 1.1]$) we obtain $\Omega_m = 0.271^{+0.030}_{-0.031}$, while if we additionally weaken the prior on $\Omega_b h^2$ (flat in the interval $[0, 0.03]$) we obtain $\Omega_m = 0.255 \pm 0.040$. Although the best fitting value of Ω_m is weakly sensitive to changes in $\Omega_b h^2$ and n_s, FIG. 3 shows that Ω_m degenerates with H_0 when the HST prior is removed. If we relax also the strong prior on H_0 (by assuming a flat prior in the interval $[40, 100]$km/s/Mpc), we find $\Omega_m = 0.22^{+0.14}_{-0.04}$. The stability of the best fitting central value Ω_m is of even more interest if contrasted to CMB results showing that it is the combination $\Omega_m h^2$ which is insensitive to the prior on the curvature of the universe.

The relevant cosmological information contained in the SDSS DR7 data can be effectively retrieved by approximating the galaxy clustering ratio $\eta_{g,R}$ in the likelihood expression (6) via the fitting formula

$$\eta_{g,R}(3R, \mathbf{p}) = 0.00712 - 0.0788x_p + 0.0981x_p^2 - 0.0538x_p^3$$

where $R = 14h^{-1}$Mpc, $x_p = 1 + \mathrm{f}_p/8.48$, and where

$$\begin{aligned}\mathrm{f}_p = \; & 3w\Omega_X - \Omega_k + 0.042\left\{w\Omega_X\left[1 - \tfrac{9}{2}(1+w)w\right] + \tfrac{\Omega_k^2 - 5\Omega_k}{2}\right\} \\ & +0.29\left\{w\Omega_X(14+3w) - 3w\Omega_X\Omega_k + \tfrac{\Omega_k^2}{2} - \tfrac{11}{3}\Omega_k\right\}\end{aligned}$$

and by further assuming $\sigma_\eta = 0.004$, independently of the cosmological model.

The advantage of probing cosmology via the ratio of second-order, one- and two-point moments of the δ_R distribution is that only a minimum amount of cosmological hypotheses, and no astrophysical nuisance parameters at all, condition the results. Of great interest is the flexibility of the method, which can still be improved along several directions. Owing to its scale-free nature, the precision of the technique could be further improved by adopting a non-linear power spectrum in eqs. (2) and (3), and by smoothing the over-density field on an even smaller scales R than that adopted throughout this analysis. The only caveat being that mass fluctuations δ_R in configuration and real spaces be simply proportional. Alternatively, the method could be applied also to large photometric redshift surveys. In this case, predictions of eq. (4) must be statistically corrected to account for the line-of-sight distortions introduced when estimating low-resolution distances from photometry. Finally, this probe enriches the arsenal of methods with which the next generation of redshift surveys such as EUCLID and BigBOSS will hunt for new physics by challenging all sectors of the cosmological model.

---

[1] L. Amendola et al., 2012, arXiv1206.1225 (2012).
[2] D. Larson et al., ApJS **192**, 16 (2011).
[3] S. Weinberg, Cosmology, Oxford University Press (2008).
[4] J. A. Frieman, M. S. Turner and D. Huterer, ARA&A **46**, 385 (2008).
[5] I. Szapudi, A. Szalay, P. Boschán, ApJ **390**, 350 (1992)
[6] F. Bernardeau, A&A **312**, 11(1996).
[7] J. Bel and C. Marinoni, MNRAS **424** 971(2012).
[8] D. Eisenstein and W. Hu, ApJ **496**, 605 (1998).
[9] C. Alcock and B. Paczynski, Nature **281**, 358 (1979) C. Marinoni and A. Buzzi, Nature **468**, 539 (2010).
[10] L. Guzzo et al. Nature, **451**,541 (2008).
[11] A. Jenkins et al., MNRAS, **321**, 372 (2001).
[12] C. McBride et al., AAS, 21342506 (2009).
[13] W. J. Percival et al. 2010 MNRAS **401**, 2148 (2010).
[14] E. Gaztanaga and A. Cabre, MNRAS **399**, 1663 (2009).
[15] R. Laureijs et al., arXiv:1110.3193 (2011).
[16] D. Schlegel et al., arXiv1106.1706 (2011).
[17] K. N. Abazajian et al., ApJS **182**, 543 (2009).

[18] M. Pettini et al., MNRAS **391**, 1499 (2008).
[19] A. Riess et al., ApJ **730**, 119 (2011).
[20] D. Eisenstein et al. **633** ,560 (2005).
[21] J. Dunkley et al. ApJS, **180**, 306 (2009).
[22] A. G. Riess et al. **699**, 539 (2009).
[23] A. G. Sanchez et al. arXiv:1203.6616 (2012).